

Fermi level pinning by defects can explain the large reported carbon 1s binding energy variations in diamond.

Michael Walter,^{1,2,3,*} Filippo Mangolini,⁴ J. Brandon McClimon,⁵ Robert W. Carpick,⁶ and Michael Moseler^{1,7,3}

¹*Fraunhofer IWM, MikroTribologie Centrum μ TC, Wöhlerstrasse 11, D-79108 Freiburg, Germany*

²*FIT Freiburg Centre for Interactive Materials and Bioinspired Technologies, University of Freiburg, Georges-Köhler-Allee 105, 79110 Freiburg, Germany*

³*Institute of Physics, University of Freiburg, Herrmann-Herder-Straße 3, D-79104 Freiburg, Germany*

⁴*Materials Science and Engineering Program and Department of Mechanical Engineering, The University of Texas at Austin, Austin, Texas 78712, USA*

⁵*Department of Materials Science and Engineering, University of Pennsylvania, Philadelphia 19104, USA*

⁶*Department of Mechanical Engineering and Applied Mechanics, University of Pennsylvania, Philadelphia, Pennsylvania 19104, USA*

⁷*Freiburger Materialforschungszentrum, Universität Freiburg, Stefan-Meier-Straße 21, D-79104 Freiburg, Germany*

(Dated: May 23, 2019)

The quantitative evaluation of the carbon hybridization state by X-ray photoelectron spectroscopy (XPS) has been a surface-analysis problem for the last three decades due to the challenges associated with the unambiguous identification of the characteristic binding energy values for sp^2 and sp^3 -bonded carbon. While the sp^2 binding energy is well established, there is disagreement for the sp^3 value in the literature. Here, we compute the binding energy values for model structures of pure and doped-diamond using density functional theory. The simulation results indicate that the large band-gap of diamond allows defects to pin the Fermi level, which results in large variations of the C(1s) core electron energies for sp^3 -bonded carbon, in agreement with the broad range of experimental C(1s) binding energy values for sp^3 carbon reported in the literature. Fermi level pinning by boron is demonstrated by experimental C(1s) binding energies of highly B-doped ultrananocrystalline diamond that are in good agreement to simulations.

I. INTRODUCTION

X-ray photoelectron spectroscopy is one of the most powerful tools for the characterization of carbon-based materials [1]. The analysis of the bonding configuration of carbon is normally carried out by XPS through the acquisition of carbon 1s (C(1s)) spectra. The spectra are often fitted with two distinct features, one assigned to threefold-coordinated (sp^2) carbon and one assigned to fourfold-coordinated (sp^3) carbon. In spite of the wide use of this analytical procedure for the quantitative evaluation of the carbon hybridization state on the basis of C(1s) XPS signals, the validity of this methodology has recently been questioned [2, 3] and still remains a matter of discussion in the literature [4].

We have recently shown that absolute XPS peak positions can be predicted by facile spin-paired DFT calculations within the frozen core approximation [5, 6]. In this approach, an empirical shift appears that can be obtained from experimental gas-phase XPS data. The main difficulty in assigning core hole energies in general, and C(1s) energies in particular, is the unambiguous definition of the reference energy. This is not the case for gas-phase investigations, where the energy of an electron in vacuum far away from the mother ion can be used

as a well-defined reference for the core electron binding energy E_B .

For solid samples the Fermi energy is usually used as the reference energy level,[7] but this energy can only be defined correctly for systems without a band gap, i.e., metals or semi-metallic systems like graphite. Accordingly, the experimental variation in C(1s) energies of semi-metal graphite is moderate and found to range from 284.28 eV to 284.63 eV [2, 3, 8–22]. Diamond, in contrast, has a very large band gap (its experimental value is 5.5 eV [23]), which hinders the consistent definition of an energy reference. Additional difficulties arise from the presence of defects, impurities, and dopants in diamond (such as nitrogen or boron[24–26]), which may pin the Fermi energy. These factors, together with effects of surface charging when acquiring XPS spectra on diamond, have resulted in the publication of a wide range of binding energy values for the C(1s) signal of sp^3 -bonded carbon (in the range of 283.25 eV - 291.35 eV) [15, 16, 27, 28]. Despite the difficulties in unambiguously assigning a characteristic binding energy value to sp^3 -bonded carbon, the quantitative evaluation of the carbon hybridization state on the basis of C(1s) XPS signals is still widely performed on the basis of fitting the C(1s) XPS spectra with two synthetic peaks, one assigned to sp^2 -hybridized carbon and one to sp^3 -hybridized carbon. Here, we use DFT calculations to compute the characteristic C(1s) binding energy values for sp^3 -bonded carbon in diamond and sp^2 -bonded carbon in graphite.

* Michael.Walter@fmf.uni-freiburg.de

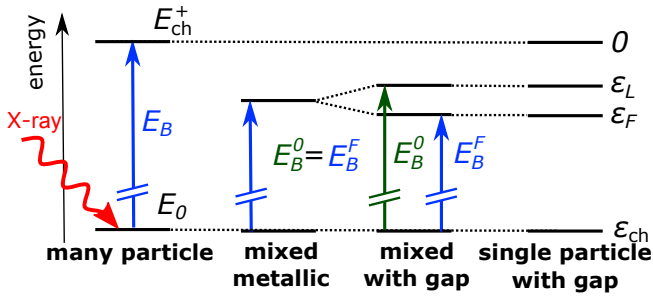


Figure 1. Schematic of many particle (capital letters) and single particle (small letters) energies involved in the definition of the core-hole binding energy corresponding to Eqs. (1-3).

II. METHODS

Our DFT calculations were carried out with the GPAW [29, 30] package, an implementation of the projector augmented wave (PAW) method [31]. The PAW method splits the Kohn-Sham wave functions into a smooth part, representable on configuration or momentum space grids, and corrections that are local near to the atoms. We use the configuration space grid implementation, and apply a grid spacing of 0.2 Å for representing the smooth part of the Kohn-Sham wavefunctions, unless noted otherwise. The exchange correlation energy was approximated by the generalized gradient correction as proposed by Perdew, Burke and Ernzerhof (PBE)[32]. We have used a spin-paired description for simplicity of band-structure analysis presented below. We have checked that the inclusion of spin does not change our results significantly. The structures were relaxed until all forces on the atoms dropped below 0.05 eVÅ⁻¹.

Lower energy atomic states can be conveniently held fixed in their atomic form within the frozen core approximation, where we include the 1s electrons for C and the diamond dopant atoms B, N, and the 1s, 2s, 2p electrons for the diamond dopant atom P in our calculations. A similar approach is adopted to describe the core hole by lowering the occupation of the relevant state in the atomic calculation by one. The resulting self-consistently obtained Kohn-Sham orbitals in the presence of the core hole are then used to construct the frozen core [30, 33, 34].

The calculation of core-hole binding energies follows the methodology developed in Ref. 5, as illustrated in Fig. 1 and is briefly summarized in what follows. XPS energies of molecules or clusters in the gas phase are well defined by the many body ground state energy E_0 and the core hole excited energy E_{ch}^+ . The latter can be approximated as the ground state of the system with a core hole in the frozen core, where the self-consistent calculation of the valence orbitals in the field of the core hole automatically takes into account relaxation effects. The photoelectrons' binding energy is then:

$$E_B = E_{\text{ch}}^+ - E_0. \quad (1)$$

XPS energies for periodic systems as modeled here have to be treated in a mixed many-body and single-particle picture. Experimentally, the core level energy is measured relative to the single particle Fermi level ε_F (smaller than zero) that is aligned to the Fermi level of the detector by holding them at a common ground[7, 35]:

$$E_B^F = E_{\text{ch}}^+ - E_0 + \varepsilon_F. \quad (2)$$

The computational difficulty of charged super-cells [36] for the description of the core ionized final state can be overcome by neutralizing the super-cell by an extra electron. This electron will locate itself in the lowest unoccupied “molecular” orbital (LUMO). Neglecting all other contributions due to the change in the electron density, this approach adds the energy ε_L to E_{ch}^+ . We obtain a binding energy in the neutralized system of the form:

$$E_B^0 = (E_{\text{ch}}^+ + \varepsilon_L) - E_0 = E_B^F + \varepsilon_L - \varepsilon_F. \quad (3)$$

For a system without a band gap, $\varepsilon_F = \varepsilon_L$ and hence conveniently $E_B^F = E_B^0$. Systems with a band gap pose several problems, however. The position of the Fermi level ε_F is not defined in these systems which prohibits a defined value for E_B^F .

III. RESULTS

In the first step, we consider the case of bulk diamond, which is the most problematic system due to its large band-gap. We model diamond by unit cells containing 64 atoms in tetrahedral configurations with the experimental lattice constant of 3.5669 Å[37] resulting in a CC bond-length of 1.55 Å. We are particularly interested in the effect of defects and impurities on the expected C(1s) value.

One of the most common impurities in natural diamond gemstones is nitrogen[24, 25] which can be present in amounts of up to 0.5 at. % [38]. Different possibilities for the presence of nitrogen are considered in the literature, where the replacement of a C atom with a N atom with or without a neighboring vacancy are believed to be the most common configurations[39]. In the former case, the P1 center[38, 40] is modeled as the replacement of a single C atom by N (C₆₃N). The nitrogen vacancy (NV) center[41] is modeled by the replacement of a single C atom by N and a neighboring vacancy (C₆₂N). The A center [39] is two neighboring N atoms (C₆₂N₂), and the N3 center[39, 42] consists of three nitrogen atoms near to a vacancy (C₆₀N₃). The B center[39] is four N surrounding a vacancy (C₅₉N₄).

Other common impurities are boron or phosphorus[43]. These elements are either present in natural diamonds (type IIb in the case of boron[9, 17]) or introduced artificially[17, 18, 21]. Boron- or phosphorus-doped structures are modeled by replacing a single C atom by B (C₆₃B) or P (C₆₃P), respectively. All model structures were relaxed to their next local minimum while the unit

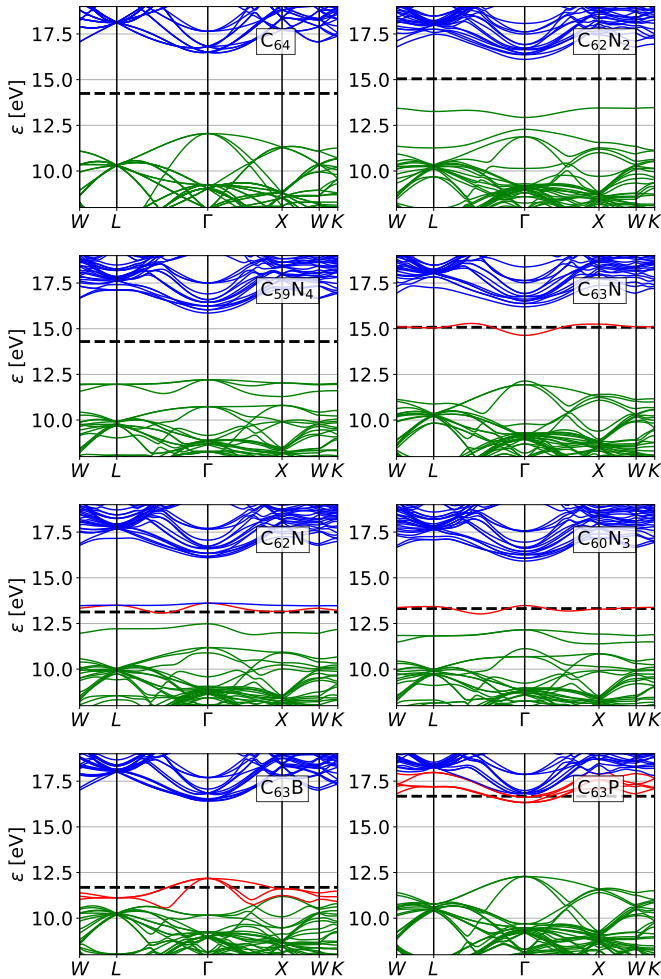


Figure 2. Band structure of diamond, pure and with defects. Fully occupied bands are colored in green, partly occupied bands in red and empty bands in blue. The broken line shows the Fermi level ε_F .

cell was kept fixed. Relaxed structures and distributions of calculated C(1s) values are depicted in Supplemental Material.

Fig. 2 shows the effect of defects on the diamond band structure. While the overall band-structure is rather similar in all cases, the defects or dopants introduce states at different positions within the diamond band gap. The gap is found to be 4.42 eV wide according to PBE[44–46] underestimating the experimental value of ~ 5.5 eV.[47, 48] This well known tendency of local and semilocal functionals to underestimate the gap can be improved by computationally more demanding hybrid functionals[45, 46], but will not affect the general effect of Fermi level pinning discussed in the following.

The two N in $C_{62}N_2$ slightly disturb a high lying unoccupied (acceptor) levels near to the conduction band edge ε_c and introduce a rather high occupied (donor) level above the valence band edge ε_v [39], thus reducing

the band gap. These levels show some variation with the wave vector in our calculation indicating interaction between periodic images. The variations are rather small (a few 100 meV) and are neglected in the following. A similar effect as in $C_{62}N_2$ is observed in $C_{59}N_4$, where mainly states slightly above ε_v are introduced. Similar to pure diamond, the Fermi level ε_F is located in the middle between the maximum of the highest occupied and the minimum of the lowest unoccupied band. An infinitesimal charge could move the Fermi energy towards the valence or the conduction band depending on its sign.

The freedom of moving the Fermi level by slight charging is not the case anymore for the other models presented in Fig. 2 as these contain an unpaired electron. There, ε_F is pinned by this half-filled state and is therefore well defined. The exact positions of the Fermi level relative to the band structure of diamond varies largely depending on the nature of the defect, however. While the half filled state is close to the conduction band in $C_{63}N$, it is found in the middle of the band gap for $C_{62}N$ and $C_{60}N_3$. The most extreme positions are found in $C_{63}B$ where the partially filled states (degenerate at the Γ -point) are near to ε_v [48, 49] and for $C_{63}P$ where partially filled states are found near to ε_c . [48]

Assuming that the C(1s) core level energy relative to the vacuum level E_B is mainly constant for carbon atoms far from any defect, the variation in ε_F will be reflected in a variation in E_B^F [c.f. eq. (2)], which is indeed the case as will be shown now.

The C(1s) XPS spectra corresponding to the defects are compared to pure diamond in Fig. 3. The unshifted spectra [broken lines, corresponding to E_B^0 in eq. (2)] of the C_{64} , $C_{62}N_2$ and $C_{59}N_4$ models are very similar in their main peak as they share the same lowest unoccupied level (c.f. Fig. 2). The spectra are different when they are corrected to ε_F located at the center of the gap (as usually assumed in semiconductors [50]) due to the different band gap values. Unshifted E_B^0 and shifted E_B^F coincide for the cases involving an unpaired electron as $\varepsilon_L = \varepsilon_F$ in these cases. The largest core level energy is found for $C_{63}N$ and the lowest energy for $C_{63}B$ as expected from the positions of the unpaired levels in Fig. 2. The main C(1s) energy in $C_{63}B$ of 284.27 eV is in good agreement to the value of 284.4 eV measured for artificially boron-doped diamond[18] and to the main peak of strongly boron-doped ultranano-crystalline diamond (UNCD) found at 284.09 ± 0.05 eV discussed in detail below.

Various side peaks appear for the different defects. In $C_{62}N_2$, there is a peak at slightly higher energy that comes from the six carbon atoms surrounding the two nitrogen atoms forming a $N(CR_3)_3$ like structure with an NC bond length of 1.45 Å very similar to the 1.46 Å in $N(CH_3)_3$. In contrast, a lower energy peak from the four carbon atoms surrounding N is found in $C_{63}N$. Here, the N has to share the bonds with four C due to symmetry. The NC bond-length is thus much longer (1.60 Å) exceeding the diamond CC bond.

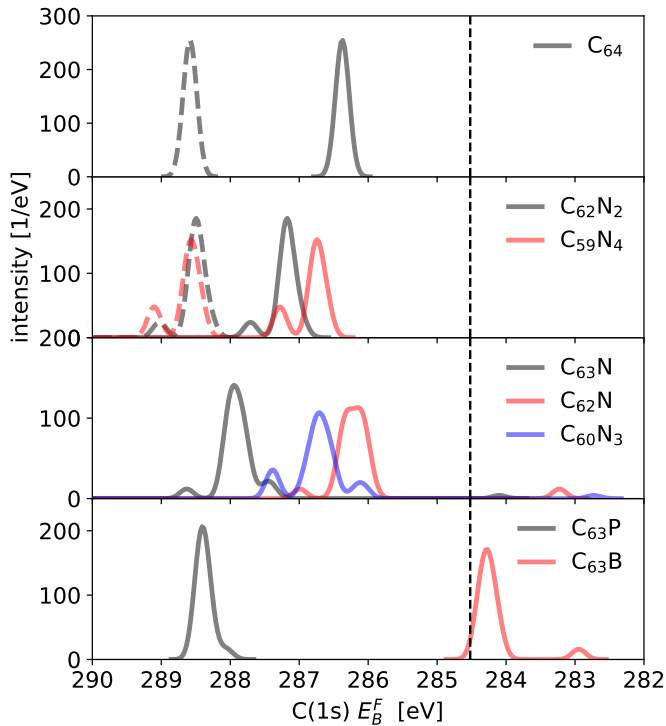


Figure 3. Absolute XPS spectra for the models derived from the C_{64} models without and with defects and impurities. The broken line is without the correction to ε_F (i.e., E_B^0) and the solid line includes this shift (i.e., E_B^F). The spectra are obtained by convoluting with Gaussians of 0.24 eV full width at half maximum (FWHM). The broken vertical line indicates graphite C(1s) energy [5].

structure	model	gap [eV]	C(1s) [eV]	shift [eV]
pure	C_{64}	4.42	286.36*	1.85
P1 center	$C_{63}N$	0	288.41	3.43
NV center	$C_{62}N$	0	286.15	1.68
A center	$C_{62}N_2$	2.64	287.17*	2.65
N3 center	$C_{60}N_3$	0	286.70	2.18
B center	$C_{59}N_4$	3.65	286.74*	2.22
B	$C_{63}B$	0	284.27	-0.25
P	$C_{63}P$	0	288.41	3.89
graphite	C_{72}	0	284.52[5]	

Table I. Pure and defected diamond model structures, their PBE band gaps, the position of their main C(1s) peak (E_B^F) and the resulting shift relative to graphite C(1s) (see also Fig. 3). The C(1s) values marked by an asterisk are corrected assuming the Fermi level to lie in the center of the band gap.

For the N impurity with a neighboring vacancy ($C_{62}N$), the lower energy peak (283.2 eV) is from the three carbons surrounding the cavity and the higher energy peak (287 eV) from the three carbons connected to nitrogen. The NC bond-length of 1.48 Å is quite similar to $N(CH_3)_3$ again.

The four carbon atoms surrounding the P atom symmetrically with a bond length of 1.70 Å in $C_{63}P$ produce the lower energy shoulder in the corresponding C(1s)

spectrum. Similarly, the lower energy peak around 283 eV in $C_{63}B$ is from the four carbon atoms surrounding B. Structurally, the B impurity atom shares four equal bonds with large CB bond length of 1.59 Å as compared to 1.55 in CC.

Besides these side peaks the main effect is the strong variation of the C(1s) peak with defect type. A defect in diamond dictates the C(1s) position of E_B^F even for carbon atoms far apart due to its influence on the Fermi level. Therefore we can conclude that diamond is a problematic system to define the sp^3 C(1s) energy as the C(1s) energy depends on the nature of defects that are omnipresent in real diamonds. This finding can contribute explaining the broad range of C(1s) values for diamond reported in the literature.[4]

We finally seek for an experimental validation of the computational analysis presented so far. Experimental XPS data were acquired on hydrogen-terminated ultrananocrystalline diamond (UNCD Aqua 25, Advanced Diamond Technologies, Romeoville, IL, USA), boron-doped ultrananocrystalline diamond (UNCD Aqua 25, Advanced Diamond Technologies, Romeoville, IL, USA),[51] and freshly cleaved highly ordered pyrolytic graphite (HOPG, grade 2, SPI Supplies, West Chester, PA, USA). Near-edge X-ray absorption fine structure (NEXAFS) spectroscopy measurements indicated that the fraction of sp^3 -bonded carbon in undoped and boron-doped UNCD was 94+/-3% and 96+/-3%, respectively [51–53]. In the present work, the X-ray source was run at 30 mA and 12 kV, whereas the analyzer was operated in constant-analyzer-energy (CAE) mode. Survey spectra were acquired with the pass energy and step size equal to 200 eV and 1 eV, respectively. For the high-resolution (HR) spectra, the pass energy and step size were, respectively, 100 and 0.05 eV (full width at half maximum (FWHM) of the peak height for the Ag 3d_{5/2} equal to 0.57 eV). The curved slit at the entrance of the hemispherical analyzer has a width of 0.8 mm. The residual pressure in the analysis chamber was always below 10^{-6} Pa. The spectrometer was calibrated according to ISO 15472:2001 with an accuracy better than ± 0.05 eV. All the XPS results reported here are mean values calculated from at least three independent measurements, with the corresponding standard deviation reported.

The DFT calculations are in good agreement with experimental XPS data acquired on undoped and B-doped UNCD shown in Fig. 4. First, the binding energy of the characteristic C(1s) peak for B-doped UNCD is lower than the binding energy of the C(1s) signal of undoped UNCD (284.09 ± 0.05 eV vs. 284.47 ± 0.05 eV, respectively in experiments) and agrees well with the 284.27 eV from DFT. Second, as in the simulation, there is a clear shoulder on the lower binding energy side in the experiment. Note that the shoulder on the high binding energy side of the experimental spectrum (286-288 eV) is caused by C-O bonds[3, 54–59] in the near-surface region. The experimental C(1s) of undoped UNCD does not agree with the calculation for pure diamond. This is not surprising with

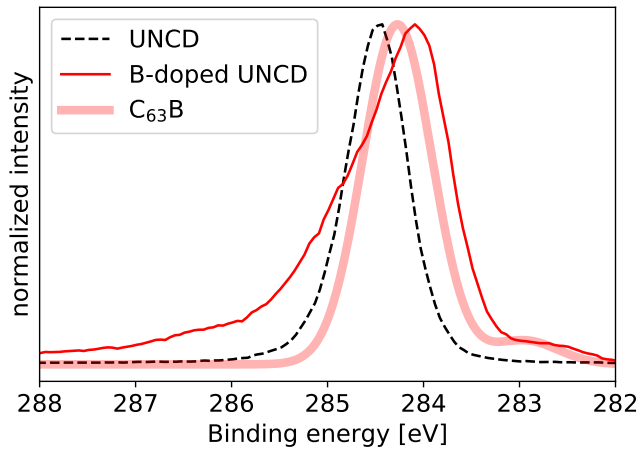


Figure 4. Experimental C(1s) spectrum of ultrananocrystalline diamond (UNCD) and B-doped UNCD compared to the calculated spectrum of the $C_{63}B$ model. The calculated C(1s) energies are convoluted by Gaussians of 0.82 eV FWHM.

respect to the large band gap of diamond and the resulting undefined Fermi level. UNCD is not single-crystal diamond and the grain boundaries contain sp^2 -carbon, defects, and are rich in hydrogen. The effect of hydrogen on the shape and position of C(1s) signal of carbon materials will be presented in a later publication. The strong influence of these defects is also inline with the observation that etching can shift the C(1s) value by several eV in UNCD films [60].

IV. CONCLUSIONS

In conclusion, we have shown that the sp^3 C(1s) binding energies determined from diamond are highly affected by the presence and nature of defects. This strong dependence of the binding energy of the characteristic C(1s) peak for sp^3 carbon on the type and number density of defects in diamond samples makes the use of diamond as reference material for XPS analysis potentially misleading. This is a consequence of the large gap, i.e. the insulating nature,[3] of undoped carbon and the resulting absence of a defined reference energy within the system. This conclusion is not restricted to diamond, but applies for XPS measurements of other wide band gap materials, where similar spreads in experimental core hole binding energies have been observed as discussed in Ref. 5.

ACKNOWLEDGMENTS

M.W. and M.M. thank G. Moras for useful discussions. Computational resources of FZ-Jülich and NEMO are thankfully acknowledged. R.W.C. acknowledges support from the U.S. National Science Foundation (NSF) through the University of Pennsylvania Materials Research Science, and Engineering Center (MRSEC) (DMR-1720530). F.M. acknowledges support from from the Welch Foundation under Grant F-2002-20190330, the Marie Curie International Outgoing Fellowship for Career Development within the 7th European Community Framework Programme under contract no. PIOF-GA-2012-328776 and the Marie Skłodowska-Curie Individual Fellowship within the European Union's Horizon 2020 Program under Contract No. 706289. J.B.M. acknowledges support of a Graduate Research Supplement for Veterans from the Directorate for Mathematical and Physical Sciences at the National Science Foundation.

-
- [1] P. K. Chu and L. Li, *Materials Chemistry and Physics* **96**, 253 (2006).
 - [2] A. Mezzi and S. Kaciulis, *Surface and Interface Analysis* **42**, 1082 (2010).
 - [3] S. Kaciulis, *Surf. Interface Anal.* **44**, 1155 (2012).
 - [4] A. Fujimoto, Y. Yamada, M. Koinuma, and S. Sato, *Analytical Chemistry* **88**, 6110 (2016).
 - [5] M. Walter, M. Moseler, and L. Pastewka, *Physical Review B* **94**, 041112(R) (2016).
 - [6] M. Walter, M. Vogel, V. Zamudio-Bayer, R. Lindblad, T. Reichenbach, K. Hirsch, A. Langenberg, J. Rittmann, A. Kulesza, R. Mitrić, M. Moseler, T. Möller, B. v. Isendorff, and J. Tobias Lau, *Physical Chemistry Chemical Physics* **21**, 6651 (2019).
 - [7] J. Riga, J.-J. Pireaux, and J. J. Verbist, *Molecular Physics* **34**, 131 (1977).
 - [8] J. Keiser and R. Kleber, *J. Appl. Phys.* **9**, 315 (1976).
 - [9] J. F. Morar, F. J. Himpsel, G. Hollinger, J. L. Jordan, G. Hughes, and F. R. McFeely, *Physical Review B* **33**, 1340 (1986).
 - [10] J. C. Lascovich, R. Giorgi, and S. Scaglione, *Applied Surface Science* **47**, 17 (1991).
 - [11] M. M. Waite and S. I. Shah, *Applied Physics Letters* **60**, 2344 (1992).
 - [12] Y. Xie and P. Sherwood, *Surf. Sci. Spectra* **1**, 367 (1992).
 - [13] G. Witek, M. Noeske, G. Mestl, S. Shaikhutdinov, and R. Behm, *Catal. Lett.* **37**, 35 (1996).
 - [14] Z. Bastl, *Collect. Czech. Chem. Commun.* **60**, 383 (1995).
 - [15] R. Graupner, F. Maier, J. Ristein, L. Ley, and C. Jung, *Phys. Rev. B* **57**, 12397 (1998).
 - [16] T. Leung, W. Man, P. Lim, W. Chan, F. Gaspari, and S. Zukotynski, *Journal of Non-Crystalline Solids* **254**, 156 (1999).
 - [17] K. Bobrov, G. Comtet, G. Dujardin, L. Hellner, P. Bergonzo, and C. Mer, *Physical Review B* **63**, 165421 (2001).
 - [18] I. Kusunoki, M. Sakai, Y. Igari, S. Ishidzuka, T. Takami, T. Takaoka, M. Nishitani-Gamo, and T. Ando, *Surface*

- Science **492**, 315 (2001).
- [19] X. B. Yan, T. Xu, S. R. Yang, H. W. Liu, and Q. J. Xue, *Journal of Physics D: Applied Physics* **37**, 2416 (2004).
- [20] K. G. Saw and J. du Plessis, *Materials Letters* **58**, 1344 (2004).
- [21] S. Ghodbane, D. Ballutaud, F. Omnès, and C. Agnès, *Diamond and Related Materials Proceedings of Diamond 2009, The 20th European Conference on Diamond, Diamond-Like Materials, Carbon Nanotubes and Nitrides, Part 1*, **19**, 630 (2010).
- [22] A. K. Schenk, K. J. Rietwyk, A. Tadich, A. Stacey, L. Ley, and C. I. Pakes, *Journal of Physics: Condensed Matter* **28**, 305001 (2016).
- [23] N. W. Ashcroft and N. D. Mermin, *Solid State Physics* (Thomson Learning, Inc., 1976) ISBN: 0030839939.
- [24] W. Kaiser and W. L. Bond, *Physical Review* **115**, 857 (1959).
- [25] S. Dannefaer, *physica status solidi (c)* **4**, 3605 (2007).
- [26] F. J. Himpsel, J. A. Knapp, J. A. VanVechten, and D. E. Eastman, *Physical Review B* **20**, 624 (1979).
- [27] K. Sawa, J. du Plessis *Materials Letters* **58**, 1344 (2004).
- [28] K. Yusaku, T. Jun, and M. Iwao, *Diamond and Related Materials* **13**, 93 (2004).
- [29] J. J. Mortensen, L. B. Hansen, and K. W. Jacobsen, *Phys. Rev. B* **71**, 035109 (2005).
- [30] J. Enkovaara, C. Rostgaard, J. J. Mortensen, J. Chen, M. Dułak, L. Ferrighi, J. Gavnholt, C. Glinsvad, V. Haikola, H. A. Hansen, H. H. Kristoffersen, M. Kuisma, A. H. Larsen, L. Lehtovaara, M. Ljungberg, O. Lopez-Acevedo, P. G. Moses, J. Ojanen, T. Olsen, V. Petzold, N. A. Romero, J. Stausholm-Møller, M. Strange, G. A. Tritsarlis, M. Vanin, M. Walter, B. Hammer, H. Häkkinen, G. K. H. Madsen, R. M. Nieminen, J. K. Nørskov, M. Puska, T. T. Rantala, J. Schiøtz, K. S. Thygesen, and K. W. Jacobsen, *J. Phys.: Condens. Matter* **22**, 253202 (2010).
- [31] P. E. Blöchl, *Phys. Rev. B* **50**, 17953 (1994).
- [32] J. P. Perdew, K. Burke, and M. Ernzerhof, *Phys. Rev. Lett.* **77**, 3865 (1996).
- [33] M. P. Ljungberg, J. J. Mortensen, and L. G. M. Pettersson, *J. Electr. Spectr. Rel. Phen.* **184**, 427 (2011).
- [34] T. Susi, M. Kaukonen, P. Havu, M. P. Ljungberg, P. Ayala, and E. I. Kauppinen, *Beilstein J. Nanotechnol.* **5**, 121–132 (2014).
- [35] T. Ozaki and C.-C. Lee, *Physical Review Letters* **118**, 026401 (2017).
- [36] F. Bruneval, J.-P. Crocombette, X. Gonze, B. Dorado, M. Torrent, and F. Jollet, *Phys. Rev. B* **89**, 045116 (2014).
- [37] D. R. Lide, ed., *CRC Handbook of Chemistry and Physics*, 85th ed. (CRC Press, Boca Raton, 2004).
- [38] E. B. Lombardi, A. Mainwood, K. Osuch, and E. C. Reynhardt, *Journal of Physics: Condensed Matter* **15**, 3135 (2003).
- [39] J. P. Goss, P. R. Briddon, R. Jones, and S. Sque, *Diamond and Related Materials 14th European Conference on Diamond, Diamond-Like Materials, Carbon Nanotubes, Nitrides and Silicon Carbide*, **13**, 684 (2004).
- [40] K. Iakoubovskii and G. J. Adriaenssens, *Journal of Physics: Condensed Matter* **12**, L77 (2000).
- [41] F. Jelezko and J. Wrachtrup, *physica status solidi (a)* **203**, 3207 (2006).
- [42] H.-C. Lu, M.-Y. Lin, S.-L. Chou, Y.-C. Peng, J.-I. Lo, and B.-M. Cheng, *Analytical Chemistry* **84**, 9596 (2012).
- [43] S. Koizumi, T. Teraji, and H. Kanda, *Diamond and Related Materials* **9**, 935 (2000).
- [44] Y. Matsuda, J. Tahir-Kheli, and W. A. Goddard, *The Journal of Physical Chemistry Letters* **1**, 2946 (2010).
- [45] L. Yang, H. Y. He, and B. C. Pan, *The Journal of Chemical Physics* **138**, 024502 (2013).
- [46] P. Rivero, W. Shelton, and V. Meunier, *Carbon* **110**, 469 (2016).
- [47] J. Ristein, *Surface Science Berlin, Germany: 4–9 September 2005 Proceedings of the 23th European Conference on Surface Science*, **600**, 3677 (2006).
- [48] K. Oyama, S.-G. Ri, H. Kato, M. Ogura, T. Makino, D. Takeuchi, N. Tokuda, H. Okushi, and S. Yamasaki, *Applied Physics Letters* **94**, 152109 (2009).
- [49] K.-W. Lee and W. E. Pickett, *Physical Review B* **73**, 075105 (2006).
- [50] P. Yu and M. Cardona, *Fundamentals of Semiconductors: Physics and Materials Properties*, 4th ed., Graduate Texts in Physics (Springer-Verlag, Berlin Heidelberg, 2010).
- [51] H. J. Zeng, A. R. Konicek, N. Moldovan, F. Mangolini, T. Jacobs, I. Wylie, P. U. Arumugam, S. Siddiqui, R. W. Carpick, and J. A. Carlisle, *Carbon* **84**, 103 (2015).
- [52] F. Mangolini, J. B. McClimon, F. Rose, and R. W. Carpick, *Analytical Chemistry* **86**, 12258 (2014).
- [53] F. Mangolini, J. B. McClimon, and R. W. Carpick, *Analytical Chemistry* **88**, 2817 (2016).
- [54] F. Arezzo, E. Severini, and N. Zaccchetti, *Surface and Interface Analysis* **22**, 218 (1994).
- [55] A. P. Dementjev and M. N. Petukhov, *Diamond and Related Materials* **6**, 486 (1997).
- [56] A. Mezzi and S. Kaciulis, *Surface and Interface Analysis* **42**, 1082 (2010).
- [57] I. Retzko and W. E. S. Unger, *Advanced Engineering Materials* **5**, 519 (2003).
- [58] J. I. B. Wilson, J. S. Walton, and G. Beamson, *Journal of Electron Spectroscopy and Related Phenomena* **121**, 183 (2001).
- [59] M. Yang, M. J. Marino, V. J. Bojan, O. L. Eryilmaz, A. Erdemir, and S. H. Kim, *Applied Surface Science* **257**, 7633 (2011).
- [60] A. V. Sumant, D. S. Grierson, J. E. Gerbi, J. A. Carlisle, O. Auciello, and R. W. Carpick, *Physical Review B* **76**, 235429 (2007).